Biomedical Optics EXPRESS

In-vivo imaging of psoriatic lesions with polarization multispectral dermoscopy and multiphoton microscopy

Dimitrios Kapsokalyvas,[1,*] Riccardo Cicchi,[1,2] Nicola Bruscino,[3] Domenico Alfieri,[4] Francesca Prignano,[3] Daniela Massi,[5] Torello Lotti,[6] and Francesco S. Pavone[1,2,7]

[1] *European Laboratory for Non-Linear Spectroscopy (LENS) University of Florence, Sesto-Fiorentino, 50019, Italy*
[2] *National Institute of Optics, National Research Council (INO-CNR), 50125, Florence, Italy*
[3] *Division of Clinical, Preventive and Oncology Dermatology, Department of Critical Care Medicine and Surgery, University of Florence, 50129, Florence, Italy*
[4] *Light4tech Firenze srl, 50018, Scandicci, Italy*
[5] *Department of Surgery and Translational Medicine, University of Florence, 50134, Florence, Italy*
[6] *Department of Dermatology and Venereology, University Guglielmo Marconi, 00193, Rome, Italy*
[7] *Department of Physics, University of Florence, 50019, Sesto Fiorentino, Italy*
**kapsokalyvas@lens.unifi.it*

Abstract: Psoriasis is a skin autoimmune disease characterized by hyperkeratosis, hyperproliferation of the epidermis and dilatation of dermal papillary blood vessels. Healthy skin (5 volunteers) and psoriatic lesions (3 patients) were visualized *in vivo*, with high contrast and resolution, with a Polarization Multispectral Dermoscope and a Multiphoton Microscope. Psoriatic features were identified and quantified. The effective diameter of the superficial blood vessels was measured at 35.2 ± 7.2 μm and the elongated dermal papillae had an effective diameter of 64.2 ± 22.6 μm. The methodologies developed could be employed for quantitative diagnostic purposes and furthermore serve as a monitoring method of the effect of personalized treatments.

OCIS codes: (180.4315) Nonlinear microscopy; (170.1870) Dermatology; (100.2980) Image enhancement; (170.6900) Three-dimensional microscopy; (170.6510) Spectroscopy, tissue diagnostics.

References and links

1. K. Wolff and T. B. Fitzpatrick, *Fitzpatrick's Dermatology in General Medicine,* 7th ed. Klaus Wolff, ed. (McGraw-Hill, 2008), pp. 2 v. (xxxv, 2402, 2136 p.).
2. R. G. Langley, G. G. Krueger, and C. E. Griffiths, "Psoriasis: epidemiology, clinical features, and quality of life," Ann Rheum Dis **64 Suppl 2**, ii18–23; discussion ii24–15 (2005).
3. M. A. Lowes, A. M. Bowcock, and J. G. Krueger, "Pathogenesis and therapy of psoriasis," Nature **445**(7130), 866–873 (2007).
4. D. Kapsokalyvas, N. Bruscino, D. Alfieri, V. de Giorgi, G. Cannarozzo, R. Cicchi, D. Massi, N. Pimpinelli, and F. S. Pavone, "Spectral morphological analysis of skin lesions with a polarization multispectral dermoscope," Opt. Express **21**(4), 4826–4840 (2013).
5. B. Masters and P. So, "Confocal microscopy and multi-photon excitation microscopy of human skin in vivo," Opt. Express **8**(1), 2–10 (2001).
6. H. G. Breunig, H. Studier, and K. König, "Multiphoton excitation characteristics of cellular fluorophores of human skin in vivo," Opt. Express **18**(8), 7857–7871 (2010).
7. J. A. Palero, H. S. de Bruijn, A. van der Ploeg van den Heuvel, H. J. Sterenborg, and H. C. Gerritsen, "Spectrally resolved multiphoton imaging of in vivo and excised mouse skin tissues," Biophys. J. **93**(3), 992–1007 (2007).
8. R. Patalay, C. Talbot, Y. Alexandrov, I. Munro, M. A. Neil, K. König, P. M. French, A. Chu, G. W. Stamp, and C. Dunsby, "Quantification of cellular autofluorescence of human skin using multiphoton tomography and fluorescence lifetime imaging in two spectral detection channels," Biomed. Opt. Express **2**(12), 3295–3308 (2011).
9. K. König, "Clinical multiphoton tomography," J. Biophotonics **1**(1), 13–23 (2008).

#206234 - $15.00 USD Received 11 Feb 2014; revised 25 Apr 2014; accepted 28 Apr 2014; published 24 Jun 2014

10. E. Dimitrow, I. Riemann, A. Ehlers, M. J. Koehler, J. Norgauer, P. Elsner, K. König, and M. Kaatz, "Spectral fluorescence lifetime detection and selective melanin imaging by multiphoton laser tomography for melanoma diagnosis," Exp. Dermatol. **18**(6), 509–515 (2009).
11. R. Cicchi, D. Kapsokalyvas, M. Troiano, P. Campolmi, C. Morini, D. Massi, G. Cannarozzo, T. Lotti, and F. S. Pavone, "In vivo non-invasive monitoring of collagen remodelling by two-photon microscopy after micro-ablative fractional laser resurfacing," J. Biophotonics (2013) DOI 10.1002/jbio.201300124.
12. R. Cicchi, D. Kapsokalyvas, V. De Giorgi, V. Maio, A. Van Wiechen, D. Massi, T. Lotti, and F. S. Pavone, "Scoring of collagen organization in healthy and diseased human dermis by multiphoton microscopy," J. Biophotonics **3**(1-2), 34–43 (2010).
13. M. J. Koehler, A. Preller, P. Elsner, K. König, U. C. Hipler, and M. Kaatz, "Non-invasive evaluation of dermal elastosis by in vivo multiphoton tomography with autofluorescence lifetime measurements," Exp. Dermatol. **21**(1), 48–51 (2012).
14. R. Cicchi, S. Sestini, V. De Giorgi, D. Massi, T. Lotti, and F. S. Pavone, "Nonlinear laser imaging of skin lesions," J. Biophotonics **1**(1), 62–73 (2008).
15. R. R. Anderson, "Polarized light examination and photography of the skin," Arch. Dermatol. **127**(7), 1000–1005 (1991).
16. S. G. Demos and R. R. Alfano, "Optical polarization imaging," Appl. Opt. **36**(1), 150–155 (1997).
17. J. Malvehy, *Handbook of Dermoscopy* (Taylor & Francis, 2006), p. 95
18. S. L. Jacques, J. C. Ramella-Roman, and K. Lee, "Imaging skin pathology with polarized light," J. Biomed. Opt. **7**(3), 329–340 (2002).
19. Y. K. Başaran, M. S. Gürel, A. T. Erdemir, E. Turan, N. Yurt, and I. S. Bağci, "Evaluation of the response to treatment of psoriasis vulgaris with reflectance confocal microscopy," Skin Res. Technol. (2014), doi:10.1111/srt.12150.
20. E. A. Wolberink, P. E. van Erp, R. T. de Boer-van Huizen, P. C. van de Kerkhof, and M. J. Gerritsen, "Reflectance confocal microscopy: an effective tool for monitoring ultraviolet B phototherapy in psoriasis," Br. J. Dermatol. **167**(2), 396–403 (2012).
21. B. R. Masters, P. T. So, and E. Gratton, "Multiphoton excitation microscopy of in vivo human skin. Functional and morphological optical biopsy based on three-dimensional imaging, lifetime measurements and fluorescence spectroscopy," Ann. N. Y. Acad. Sci. **838**(1 ADVANCES IN O), 58–67 (1998).
22. L. H. Laiho, S. Pelet, T. M. Hancewicz, P. D. Kaplan, and P. T. So, "Two-photon 3-D mapping of ex vivo human skin endogenous fluorescence species based on fluorescence emission spectra," J. Biomed. Opt. **10**(2), 024016 (2005).
23. B. Schmid, J. Schindelin, A. Cardona, M. Longair, and M. Heisenberg, "A high-level 3D visualization API for Java and ImageJ," BMC Bioinformatics **11**(1), 274 (2010).
24. S. Hern, A. W. Stanton, R. H. Mellor, C. C. Harland, J. R. Levick, and P. S. Mortimer, "In vivo quantification of the structural abnormalities in psoriatic microvessels before and after pulsed dye laser treatment," Br. J. Dermatol. **152**(3), 505–511 (2005).
25. J. Hegyi, V. Hegyi, G. Messer, P. Arenberger, T. Ruzicka, and C. Berking, "Confocal laser-scanning capillaroscopy: a novel approach to the analysis of skin capillaries in vivo," Skin Res. Technol. **15**(4), 476–481 (2009).
26. S. González, M. Rajadhyaksha, G. Rubinstein, and R. R. Anderson, "Characterization of psoriasis in vivo by reflectance confocal microscopy," J. Med. **30**(5-6), 337–356 (1999).
27. M. Ardigo, C. Cota, E. Berardesca, and S. González, "Concordance between in vivo reflectance confocal microscopy and histology in the evaluation of plaque psoriasis," J. Eur. Acad. Dermatol. Venereol. **23**(6), 660–667 (2009).
28. E. A. Wolberink, P. E. van Erp, M. M. Teussink, P. C. van de Kerkhof, and M. J. Gerritsen, "Cellular features of psoriatic skin: imaging and quantification using in vivo reflectance confocal microscopy," Cytometry B Clin. Cytom. **80**(3), 141–149 (2011).
29. R. Archid, A. Patzelt, B. Lange-Asschenfeldt, S. S. Ahmad, M. Ulrich, E. Stockfleth, S. Philipp, W. Sterry, and J. Lademann, "Confocal laser-scanning microscopy of capillaries in normal and psoriatic skin," J. Biomed. Opt. **17**(10), 101511 (2012).
30. K. König, H. G. Breunig, R. Bückle, M. Kellner-Höfer, M. Weinigel, E. Büttner, W. Sterry, and J. Lademann, "Optical skin biopsies by clinical CARS and multiphoton fluorescence/SHG tomography," Laser Phys. Lett. **8**(6), 465–468 (2011).
31. H. G. Breunig, R. Bückle, M. Kellner-Höfer, M. Weinigel, J. Lademann, W. Sterry, and K. König, "Combined in vivo multiphoton and CARS imaging of healthy and disease-affected human skin," Microsc. Res. Tech. **75**(4), 492–498 (2012).
32. E. Ayroldi, A. Bastianelli, L. Cannarile, M. G. Petrillo, D. V. Delfino, and A. Fierabracci, "A pathogenetic approach to autoimmune skin disease therapy: psoriasis and biological drugs, unresolved issues, and future directions," Curr. Pharm. Des. **17**(29), 3176–3190 (2011).
33. E. D. O. Roberson and A. M. Bowcock, "Psoriasis genetics: breaking the barrier," Trends Genet. **26**(9), 415–423 (2010).
34. W. Weger, "Current status and new developments in the treatment of psoriasis and psoriatic arthritis with biological agents," Br. J. Pharmacol. **160**(4), 810–820 (2010).

#206234 - $15.00 USD Received 11 Feb 2014; revised 25 Apr 2014; accepted 28 Apr 2014; published 24 Jun 2014

35. P. I. Spuls, L. L. A. Lecluse, M. L. N. F. Poulsen, J. D. Bos, R. S. Stern, and T. Nijsten, "How Good Are Clinical Severity and Outcome Measures for Psoriasis?: Quantitative Evaluation in a Systematic Review," J. Invest. Dermatol. **130**(4), 933–943 (2010).
36. M. Suárez-Fariñas, K. R. Shah, A. S. Haider, J. G. Krueger, and M. A. Lowes, "Personalized medicine in psoriasis: developing a genomic classifier to predict histological response to Alefacept," BMC Dermatol. **10**, 1 (2010).
37. R. T. Woolf and C. H. Smith, "How genetic variation affects patient response and outcome to therapy for psoriasis," Expert Rev. Clin. Immunol. **6**(6), 957–966 (2010).

1. Introduction

Psoriasis is a common human skin disease which is seen worldwide, in all races, and both sexes [1]. It is estimated that affects around 2-3% of the Western populations [2] and the etiology is still unknown. It has been recognized from the ancient times, although it was sometimes mistaken for leprosy. It is a chronic condition with a variable course, periodically improving and worsening and it is not contagious. It occurs when the immune system sends out faulty signals that speed up the growth cycle of skin cells. As a consequence there is an excessive growth and abnormal differentiation of keratinocytes, which macroscopically results to increased redness and scaling of the skin. Until recently it was believed to be incurable. However, recent studies show that there are new therapies emerging which target the molecular origin of the disease and could lead to its cure [3]. Due to the intense research focusing on the treatment and the cure of this chronic disease it is fundamental to have the means of monitoring the effect of various treatments from the macroscopic down to the microscopic level of organization of skin.

For this purpose two complementary custom built *in vivo* optical imaging modalities for the application on human skin were employed: a Polarization Multispectral Dermoscope (PMD) and a Multiphoton Microscope (MM). The PMD focuses on the macroscopic imaging of skin lesions. The potential of this device has been already demonstrated on imaging of melanocytic and non-melanocytic skin lesions [4]. This device produces enhanced contrast images of the blood vessel morphology, melanin localization and the single-scattering profile of a skin lesion. In the present study the PMD was employed mainly for the visualization of the dilated psoriatic blood vessels.

High resolution microscopic imaging was performed with a Multiphoton Microscope (MM). Autofluorescence signal of endogenous fluorophores such as NADH, FAD, keratin, lipofuscin, elastin, collagen, melanin, and porphyrines can be detected [5–8]. These signals encode information on the content and the biochemical environment of the skin tissue, therefore can be sensitive on functional information unattainable with other techniques. The advantages of this technique have already been demonstrated on healthy skin but also on various skin diseases [9–13]. For this reason we developed a MM capable of recording the spectral response of the tissue and assess the differences in the cellular environment between healthy and diseased skin which has already been used *in vivo* and *ex vivo* applications [11, 14]. In the present study, the focus is mainly on the morphological characteristics of the skin epithelium and the papillary dermis. In the epithelium, contrast comes from the autofluorescence signal whereas in the papillary dermis contrast is based on the second-harmonic generation (SHG) signal from collagen fibers. The characteristic morphological differences that can be observed between healthy and psoriatic skin are already established by histopathological examinations [1, 3]. In the present study these morphological differences were visualized *in vivo* with the developed systems and in a non invasive mode. Moreover, these observations were quantified and could be used for monitoring their course during topical, phototherapy or systemic treatments.

#206234 - $15.00 USD Received 11 Feb 2014; revised 25 Apr 2014; accepted 28 Apr 2014; published 24 Jun 2014

2. Materials and methods

2.1 Polarization Multispectral Dermoscope

The details of the Polarization Multispectral Dermoscope (PMD) have been presented elsewhere [4]. In brief, the major components of PMD are the dermoscope head, the electronics control box and a computer for storing and processing the acquired images. The dermoscope head houses three types of high luminance LEDs, emitting in the blue (470 nm), green (530 nm) and red (625 nm). Additionally, a polarizer in the illumination and an analyzer in the detection path enable polarization-gated imaging. Images are recorded by a CMOS color camera. Images in the cross-polarization configuration under blue, green and red illumination are recorded. The cross-polarization configuration allows imaging of deeper laying structures [15, 16]. When, all three LEDs types are combined, a white illumination image of the lesion is recorded and serves as the equivalent of a classical dermoscopic image. Finally an image in the co-polarized configuration under blue illumination is acquired. The spectral images are processed for enhancing the morphological features. Blood vessel morphology is enhanced when the image acquired under red illumination is subtracted from the one acquired under green illumination and the difference is divided by their sum. The result is the Blood Contrast image where hemoglobin and therefore blood vessels are visualized with high contrast. Structures with different scattering properties are enhanced in the Scattering Contrast image. This image is produced when the cross-polarized imaged is subtracted from the co-polarized image under blue illumination. The resulting image has high contrast for superficially scattering structures.

The Blood Contrast images produced after processing the PMD images are used for the quantification of the blood vessel superficial size. The analysis is performed with a routine developed in MATLAB 7.1 (Mathworks Inc, Natick, MA, USA, 2007). The first step in this analysis is the segmentation of the Blood Contrast image for highlighting blood vessels. This is achieved by creating a window of 10x10 pixels which propagates along all the pixels of the images, excluding 10 pixels on all sides of the image. The diameter of most vessels is less than 10 pixels^2 and the background intensity provides sufficient contrast. If the central pixel of the window has a value below the average value of the borders of the window then this pixel is identified as a blood vessel pixel and assigned the value of 1. Pixels that are not identified as vessels are attributed the value zero. The routine creates a binary image where the contrast of blood vessels is maximum (Fig. 2(g)). Subsequently, the routine identifies each single blood vessel and measures its cross-sectional surface. Hairs are excluded from the segmentation routine by removing structures that are more than 20 pixels long. Finally the number of blood vessels in each image is calculated and the average surface of the superficial blood vessels calculated.

2.2Multiphoton microscope setup

A custom MM ((Fig. 1(b)) specifically for the purpose of *in vivo* skin imaging was developed. The laser source is a Chameleon Ultra II (Coherent Inc, Santa Clara, CA, USA) mode-locked Ti:Sapphire laser (140 fs, 80 MHz repetition rate). A half-wavelength waveplate ($\lambda/2$) (Thorlabs, Newton, NJ, USA), coupled with a polarizing beam splitter (PBS, Thorlabs, Newton, NJ, USA) are employed for controlling the laser power. A beam shutter controls the transmission of the beam. A telescope (L1, f = 100mm, L2, f = 200mm) is used to collimate and enlarge the beam in order to fit with the galvo mirrors diameter. The laser beam is guided inside a 7 mirror articulated arm (El.En Group, Calenzano, Italy) which is connected with the microscope. This configuration permits the free movement of the microscope head while maintaining the laser beam aligned and centered inside the arm itself.

The microscope head consists of two stages: the excitation stage and the detection stage (Fig. 1(a)). This configuration allows the minimization of the microscope head size and facilitates its movement. Through the articulated arm the beam is delivered to the scanning

#206234 - $15.00 USD Received 11 Feb 2014; revised 25 Apr 2014; accepted 28 Apr 2014; published 24 Jun 2014

head inside the excitation stage. The scan head is composed of two galvo mirrors (G1222, Galvoline, Italy). The beam will subsequently propagate the scanning lens (SL, f = 40 mm) and the tube lens (TL, f = 150 mm). The objective lens is mounted at the end of the excitation stage. It is mounted on a movable mount driven by a DC motor (M-501, Physik Instrumente GmbH, Karlsruhe, Germany), which controls the axial movement of the objective and therefore the focal depth inside the sample. Two objective lenses are used on this microscope. One with high magnification and high numerical aperture (NA) for resolving the cellular details of the epidermis (Fluar 40X, N.A. 1.3, W.D 0.17mm, oil immersion, Carl Zeiss MicroImaging GmbH, Germany), and another one with lower magnification but longer working distance (WD), which is used for imaging deep inside the skin (XLUM 20X, N.A. 0.9, WD: 2mm, water immersion, Olympus Co., Japan). Between the objective lens and the tube lens a dichroic mirror (D1, FF665-Di02-25x36, Semrock, Rochester, NY, USA) is mounted at a 45° position in order to allow the excitation beam to pass through but reflect the signal to the detection stage.

The detection stage is mounted exactly above the excitation stage. A one-inch wide aperture above the dichroic mirror allows the transmission of the signal in the detection stage. A cut-off filter (CF), (FF01-680/SP-25, Semrock, Rochester, NY, USA) blocks any reflected laser light. A mirror directs the signal to the PMT (H7422-40, Hamamatsu Photonics, Japan). The PMT is connected to a custom made integration and amplification circuit which is mounted outside and away from the microscope head. A lens (L5, f = 50 mm) focuses the signal to the effective area of the PMT.

All electronic systems are connected to an I/O acquisition board (PCI-MIO-16E, National instruments, Austin, TX, USA). The acquisition board is housed inside the computer and controlled by a custom made LabVIEW routine. All the electronic subsystems of the microscope are controlled by a custom made interface developed in LabVIEW 7.1 (National instruments, Austin, TX, USA). This enables the remote operation of the microscope.

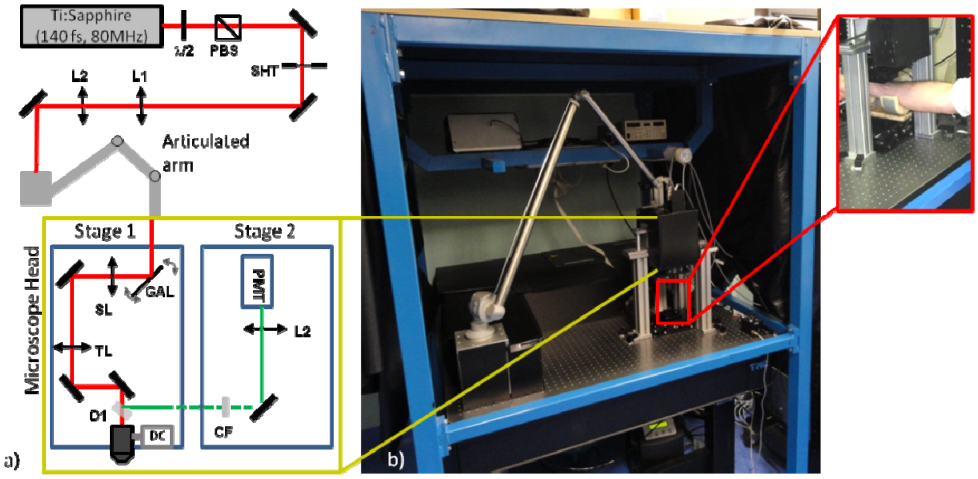

Fig. 1. Multiphoton Microscope, a) A schematic view of the experimental setup, b) A photograph of the Multiphoton Microscope where the articulated arm and the microscope head are visible. In the inset, a magnified photo of the configuration used for in-vivo imaging.

2.3 Examined volunteers

All the measurements were performed in the Dermatology Clinic of the University of Florence. The study included 8 Caucasians volunteers, 5 healthy and 3 affected with psoriasis. The volunteers were selected among individuals that visited the Clinic for a scheduled examination. The study was approved by the Institutional Review Board of the University of Florence, and conducted according to the tenets of the Declaration of Helsinki. Written

#206234 - $15.00 USD Received 11 Feb 2014; revised 25 Apr 2014; accepted 28 Apr 2014; published 24 Jun 2014

informed consent was obtained from all study participants after detailed explanation of the study. Five healthy volunteers and three with psoriatic lesions, with skin phototypes II and III, were examined with both the devices developed. All the measurements were performed on the forearm of the subjects. The three patients appeared with the most common clinical variant of psoriasis, psoriasis vulgaris. They presented erythemato-squamous plaques, oval and round shaped, variable in size and typically affecting elbows, knees and other body parts by a symmetrical pattern. Since the presence of thick scales would have impeded the examination by the multispectral dermoscope and mainly by the multiphoton microscope, we preferred to conduct our study, imaging and evaluating only the plaques characterized by a mild hyperkeratosis and therefore minimally scaly. The courses of their diseases were chronic, affecting them from several years through alternating periods of relapses and remissions; they had followed topical and systemic therapies too.

For the dermoscopic examination, the dermoscope head was positioned in contact to the lesion. A drop of water was used as an index matching fluid. Cross- and co- polarized images at different LED configurations were acquired with exposure of 0.2 s for each setting and the total acquisition time was less than 2 s. For the MM examination, a custom mount holding the forearm was positioned under the microscope objective (Fig. 1(b)). In front of the objective a special metallic mount ensured that the surface in contact was flat and an opening in the centre, where a cover slip was positioned, allowed the excitation, the autofluorescence and the SHG signal to pass through. Two different configurations were used for imaging. Imaging of the skin epithelium was performed with a high NA objective (Zeiss NA:1.3) and the excitation was at 740 nm with power at the focus between 20 and 40 mW depending on the depth. Imaging of the connective tissue was performed with long working distance objective (Olympus NA:0.9, 2 mm working distance) and the excitation was at 900 nm with power at the focus between 40 and 60 mW depending on the depth. Pixel resolution in both configurations was 512 × 512 pixels, with a pixel dwell time of 20 μs and 50 KHz pixel scan speed.

The PMD with a relatively big Field of View (FOV) of 8 × 6 mm offers a general view of a lesion. In contrast, the MM has a much smaller FOV but offers much higher resolution where subcellular features in the epidermis and the collagen fibers in the dermis can be resolved. When imaging the epidermis with the 40X Zeiss objective the MM offers a FOV of 200 × 200 μm and when imaging the dermis with the 20X Olympus objective the FOV is 400 × 400 μm.

3. Results

3.1 Polarization Multispectral Dermoscope results

The PMD was employed for the *in vivo* dermoscopic imaging of psoriatic lesions. Representative images of a psoriatic lesion and healthy skin, for comparison, are presented in Fig. 2. In Figs. 2(a)-2(c) a healthy skin region from the dorsal forearm of a 35 year male is presented. Dermoscopically it appears homogeneous (Fig. 2(a)), in the Blood Contrast image (Fig. 2(b)) small blood vessels encoded with dark grey become visible and in the Scattering Contrast image (Fig. 2(c)) the wrinkle network becomes visible. The psoriatic lesion from a 35 year old female dermoscopically (Fig. 2(d)) has the common characteristics of psoriasis, which is pink-red patches, with red dots of variable size and density [17]. Some black hairs are still visible in the image. Processing of the images acquired with the PMD revealed, with higher contrast, the dermoscopic characteristics of psoriasis. Dilated blood vessels appear as dark structures in Fig. 2(e). Blood vessels in psoriasis are characterized by elongated, tortuous capillaries. The details of these capillaries can be visualized in certain degree on the inset of Fig. 2(e). This characteristic vascular structure corresponds to the dilated blood vessels, which is the normal inflammatory response of the skin to the abnormal cell growth.

#206234 - $15.00 USD Received 11 Feb 2014; revised 25 Apr 2014; accepted 28 Apr 2014; published 24 Jun 2014

The scattering profile of the lesion can be seen in the Scattering Contrast image (Fig. 2(f)). Here contrast comes from the intensity of single scattered photons [4, 18]. Regions with lower back-scattering potential, such as wrinkles, appear darker. The characteristic feature of Fig. 2(c) is the absence of a wrinkle network, a feature normally seen in healthy skin (Fig. 2(c)). There are sporadically some wrinkles but they are isolated and disconnected from each other. This is the result of the abnormal differentiation of keratinocytes and the lack of the ability to organize and form an ordered structure as seen in healthy skin. Also, some other dark structures which appear as black parallel lines are indicated with a circle in Fig. 2(f). It is still not clear what the histological correspondence of these structures is.

The Blood Contrast images reveal with high contrast the morphology of blood vessels and therefore these images are used for the quantification of their size in healthy and psoriatic skin. The number of blood vessels in psoriatic lesions as well as for healthy skin varied greatly with values ranging from 1000 to 4000 vessels in a surface of 51.2 mm^2, which is the field of view. The mean cross sectional vessel size in psoriasis remains fairly constant with a mean value of around 974.4 ± 40.5 μm^2 whereas the mean size of blood vessels in healthy skin was much smaller with a measured mean value of 532.4 ± 45.9 μm^2 ($p<0.001$)..The percent difference of mean vessel size between psoriatic and healthy skin was 83%, which effectively means that psoriatic vessels were almost double in size compared to healthy skin. This observation is important because vcascularization correlates with inflammation. Moreover following a treatment vascularization [19] and vessel size [20] have been reported to decrease, as it has been observed with reflectance confocal microscopy and therefore vessel size could become a diagnostic descriptor for psoriasis.

Subsequently, image Fig. 2(h) is produced with the merging of the segmented image Fig. 2(g) and the Blood Contrast result of Fig. 2(e) so the segmentation result can be better visualized. Figure 2(i) is produced by merging the segmented image of Fig. 2(g) with the scattering contrast result of Fig. 2(f). In Fig. 2(i) becomes obvious that blood vessel do not colocalize with the dark structures of the Scattering Contrast result. Since blood capillaries do not infiltrate in these regions it is possible that these structures correspond to regions of epidermal proliferation. The diagnostic significance of the scattering contrast result for the case of Psoriasis is still not clear as this is a newly developed methodology. However it provides new type of information not available with conventional dermoscopy and its significance has to be evaluated in a bigger scale clinical study.

#206234 - $15.00 USD Received 11 Feb 2014; revised 25 Apr 2014; accepted 28 Apr 2014; published 24 Jun 2014

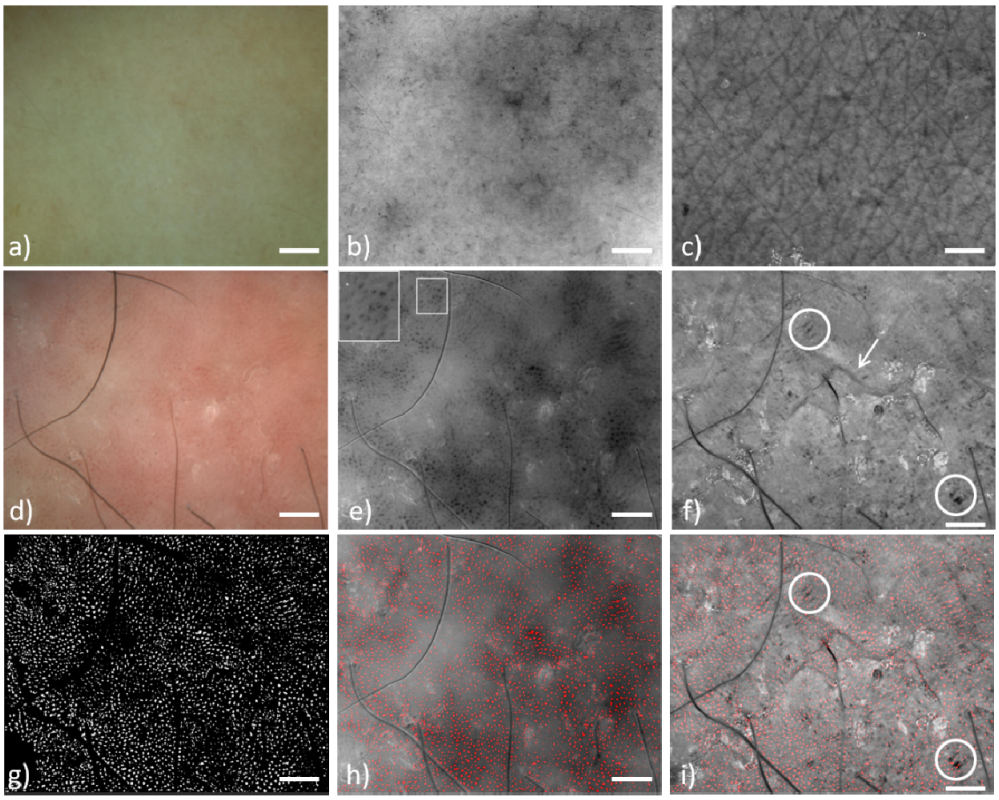

Fig. 2. Polarization Multispectral Dermoscope images. Healthy skin (a-c). Psoriasis (d-i). a)Dermoscopic white light image, b) Blood Contrast, blood vessels are encoded dark grey, small ones are visible c) Scattering Contrast, well defined wrinkle network is visible, d) Dermoscopic white light image where homogeneous red dots with some patches of pink to bright red are visible, e) Blood Contrast image, bigger blood vessels are visible. Inset: magnified vessel details, f) Scattering Contrast image. The wrinkle network is completely absent. Arrow: wrinkle, circles: dark parallel structures g) The vessel segmentation image, f) Blood Contrast image merged with the segmented image, i) Scattering Contrast image merged with the segmented image, blood vessels do not colocalize with the characteristic dark parallel structures of psoriasis. (Scale bar: 1mm)

3.2 Multiphoton microscope results

The microscopic imaging was performed on the dorsal forearm and in the same region of the forearm as where the dermoscopic images were taken from. The microscope images of the same case examined in the previous section are presented. Imaging of the epidermis and the dermis was performed under different conditions. For the epidermis, the aim was on increasing the detected autofluorescence signal while maintaining high resolution, high enough to resolve subcellular structures. For the dermis the aim was to acquire images from deeper layers and with a larger field of view.

3.2.1 Epidermis

High resolution images of the two-photon autofluorescence of the epidermis were acquired with a high NA objective (Zeiss, NA: 1.3, 40X). Autofluorescence in this part of the skin comes mainly from NADH, FAD, keratin, melanin and lipids [9, 21]. However at the excitation wavelength of 740 nm used, the dominant fluorophore is NADH which is abundant in the cytoplasm [21, 22]. The nucleus does not fluoresce therefore it appears as a black round object in the images.

#206234 - $15.00 USD Received 11 Feb 2014; revised 25 Apr 2014; accepted 28 Apr 2014; published 24 Jun 2014

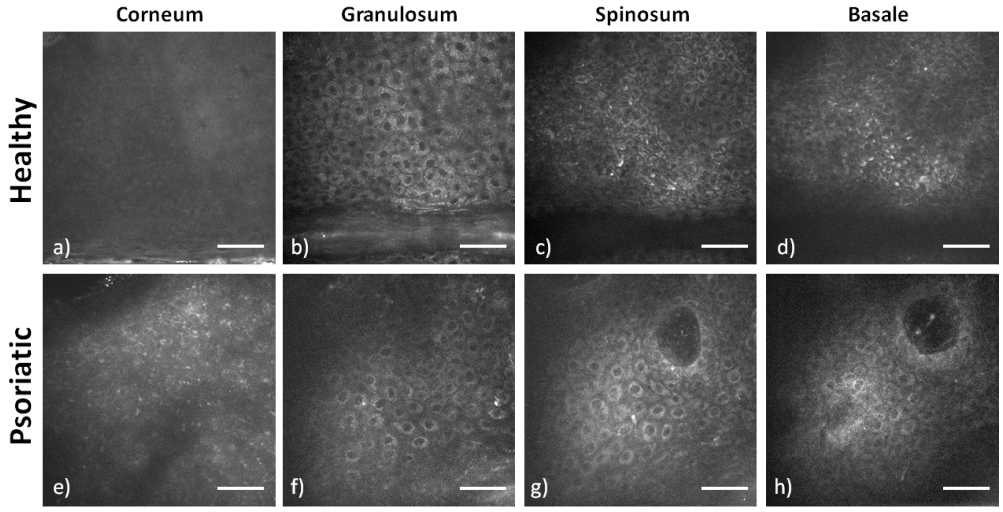

Fig. 3. Two photon autofluorescence images of the layers of the epidermis. The images are from the dorsal forearm of healthy (a-d) and psoriatic (e-h) skin. Scale bars: 50 μm

A typical set of images from a healthy and psoriatic epidermis can be seen in Fig. 3. The images are a stack from the dorsal forearm of a 30 years old healthy male (Figs. 3(a)-3(d)) and a 35 year old female with Psoriasis (Figs. 3(a)-3(d)). Imaging sequence begins below the surface of the corneum for safety and practical reasons. Signal from the surface of the corneum is very strong. This can cause the shutdown of the PMT which is adjusted for detecting a very low autofluorescence signal from the epidermis. Since the acquisition of all image sections is automated, imaging of the skin surface is excluded. In healthy skin the lower level of the stratum corneum (Fig. 3(a)) fluorescence appears to be uniform without a characteristic morphology, whereas in psoriatic skin a characteristic punctuated pattern appears (Fig. 3(e)). The origin of this signal, which does not resemble to cell cytoplasm or to the corneum, is not unequivocally identified. This unusual morphology is most probably due to the incompletely differentiated keratinocytes. Cells do not lose their nuclei as in healthy skin and maybe they still retain some components and functions not found in this layer in healthy skin. This morphology is seen also in the other cases of psoriasis but in none of the cases of healthy skin. Therefore it is believed to be a characteristic feature of psoriasis.

In the stratum granulosum the healthy epidermis is constituted of large cells with the characteristic granular morphology in the cytoplasm (Fig. 3(b)). The psoriatic stratum granulosum in most of the cases is very thin and in some cases is even absent. Here, the cells of the stratum granulosum (Fig. 3(f)) have a very small cytoplasmic area. In the stratum spinosum of healthy skin cells are densely packed and have the characteristic spiny morphology (Fig. 3(c)). Stratum spinosum is a relatively extended layer and the cells may resemble those of the stratum granulosum especially in size. However, fluorescence from the cytoplasm is uniform. In psoriatic spinosum (Fig. 3(g)) cells appear with a very small cytoplasmic area and additionally nuclei appear bigger compared to healthy cells. The packing also is very sparse with longer distances between adjacent cells. Quantification of the increased extracellular space is challenging since the contrast from the images is not always high enough for successful segmentation. However, the nucleus to cytoplasm surface ratio has been quantified, based on manual segmentation, on selected images, with high enough contrast, from the upper layers of the stratum spinosum. It was found to be 0.16 ± 0.02 for healthy skin and 0.23 ± 0.03 for psoriasis ($p<0.001$). Careful selection on the analyzed images has to be made since nucleus to cytoplasm ratio decreases as we move deeper in the epidermis for both cases.

#206234 - $15.00 USD Received 11 Feb 2014; revised 25 Apr 2014; accepted 28 Apr 2014; published 24 Jun 2014

In the stratum basale of healthy skin (Fig. 3(d)) cells have even smaller cross-sectional surface, they are densely packed and they have strong fluorescent signal. The psoriatic stratum basale (Fig. 3(h)) is not well visible in a single image section due to its wavy morphology and deep epidermal proliferation. However around the formation of the papillae it is possible to identify the basal layer. Again cells appear with a very small cytoplasmic area, however packing is denser compared to stratum spinosum. Another characteristic feature is the presence of dermal papillae that infiltrate inside the epidermis. In healthy skin occasionally there can be a papilla infiltrating inside the epidermis but it never reaches so near to the surface. In psoriatic lesions papillae infiltrate deep in the epidermis as it can be seen in the Fig. 3(g) and 3(h).

3.2.1 Papillary dermis

Imaging of the Papillary dermis is performed with an Olympus objective (Olympus, NA:0.95, 20X, WD: 2 mm), which offers longer working distance and bigger FOV. Typically the FOV of the images acquired is 400 × 400 μm^2. Anatomically the dermal layer begins at around 80 μm below the surface of the skin. At this depth the attenuation of the excitation beam due to scattering or absorption can be significant. In order to image deeper layers of the dermis the use of longer excitation wavelengths was investigated. Fluorescence reduces at longer wavelengths but SHG increases significantly. Therefore the contrast mechanism used for the imaging of the dermis was the SHG from collagen. This allows imaging of dermis as deep as 200 μm below the skin surface. SHG is an adequate contrast mechanism because almost 75% of dermis is composed of collagen, therefore the greater part of dermis is possible to be imaged. The morphology of collagen fibers can be well delineated. However the fluorescence contribution is very low and cellular information cannot be acquired. The optimal wavelength used for imaging dermal collagen was 900 nm. Although collagen has a higher SHG cross-section at shorter wavelengths (in the 800 nm – 840 nm range), we measured a higher SHG signal using 900 nm. This is probably due to the fact that collagen is located at a depth of at least 80-100 μm from tissue surface and 900 nm penetrates deeper compared to shorter wavelengths.

A characteristic case from the dorsal forearm of a 30 years old male is presented in Fig. 4(a). The start of imaging depth is around 85 μm below the surface. In the first layers of dermis collagen fibers have small diameter and they form a very complex network. They have a curly appearance and they are very dense. The diameter is small (around or less than 1 μm). They form a collagen mesh. In the first layers of dermis dermal papillae dominate the images and their density is high. Dark regions in the images are occupied by small epidermal proliferation. Fluorescence at this excitation wavelength (900 nm) is very weak and therefore epidermal layers are not visible. At a depth of 150 μm below the surface most of the dermal papillae disappear in the dense collagen network. At deeper layers collagen fibers gradually increase in size and the collagen network appears with better contrast. The network is less complex and the direction of the fibers more ordered. At the depth of 180 μm the quality of the image starts to degrade due to scattering.

The images of papillary dermis of a psoriatic lesion from the dorsal forearm of a 35 year old female are presented in Fig. 4(b). The start of imaging depth is around 85 μm below the surface. In the more superficial layers the formation of the papillae is observed. The density of the papillae is high. Deeper in the papillary dermis the presence of papillae is still evident and the space around them starts to be filled with collagen which signifies that the main dermal layer is reached. At a depth of 170 μm below the surface of the skin the dermis starts to have a morphology that is similar to that of healthy skin. However the fine collagen network of interwoven curly fibers below the dermo-epidermal junction which is seen in healthy skin is not visible in psoriasis. It appears that the formation of papillae in psoriasis starts at depths around 170 μm below the skin surface whereas in healthy skin the formation starts at a depth of around 115 μm. This also means that epidermal proliferations, which

#206234 - $15.00 USD Received 11 Feb 2014; revised 25 Apr 2014; accepted 28 Apr 2014; published 24 Jun 2014

occupy the dark space in the images of Fig. 4, reach deeper than 170 μm in psoriasis whereas in healthy skin this depth is around only 115 μm.

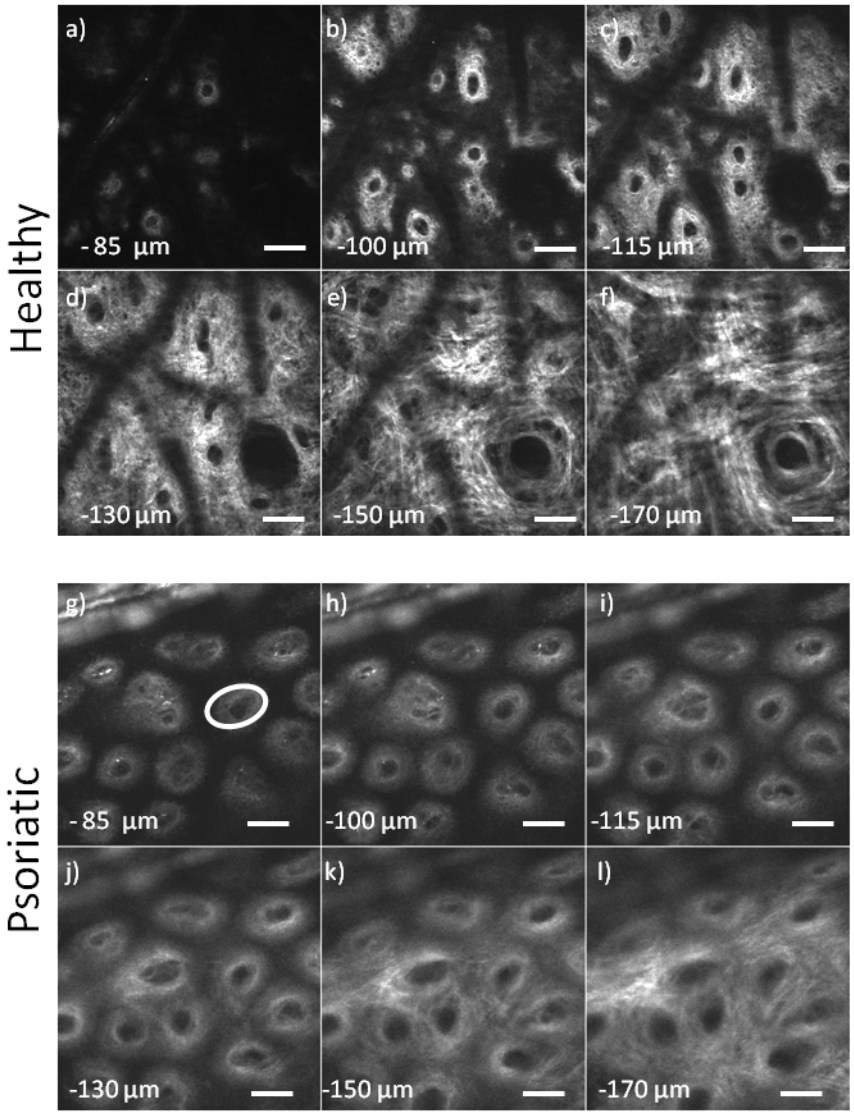

Fig. 4. SHG images of the dermis, a-f) Images from healthy papillary dermis, g-l) Images from psoriatic papillary dermis, the ellipse in g) marks the surface of the papilla measured (scale bars: 50 μm).

The characteristic feature of these images (Fig. 4(g)-4(l)) is the elongated dermal papillae. This feature becomes better visible in the 3D reconstruction of this part of the skin. To accomplish this, volume stacks with 5 μm step are recorded and the *ImageJ* plug-in 3D Viewer [23] is used to produce the 3D reconstruction. The result is presented in Fig. 5 where the elongated papillae are clearly seen. The 3D volumes reconstructed can be rotated freely at any angle. In Fig. 5(a) and 5(b) can be seen the reconstructed volumes, of healthy and psoriatic skin, from the top view. In Figs. 5(c) and 5(d) the volumes are rotated at 30° degrees in the y-z plane, so that the side view of the volumes is better visible. In those images the diameter and the length of the papillae is better visible. Examination of the 3D images reveals that some of these papillae in psoriasis have a length of around 100 μm, which is much longer

#206234 - $15.00 USD Received 11 Feb 2014; revised 25 Apr 2014; accepted 28 Apr 2014; published 24 Jun 2014

than the length of healthy papillae, which is around 30 µm. Additionally, the psoriatic papillae are dilated whereas in healthy skin papillae are much smaller. In order to quantify the differences of the dermal papillae observed in psoriatic lesions the cross sectional surface that they occupy in healthy and psoriatic lesions was measured. The papillae surface was calculated on the images presented in Fig. 4 or similar. In order to establish a consistent measurement method for the papillae surface its surface was measured at around 10 µm below its tip. The papillae are not circular, they are closer to an ellipse so it was more accurate to measure the surface they occupy rather than a diameter. However the establishment of a more intuitive measure of their size was pursued and therefore based on the surface measurements the size of the diameter of a circle that would occupy the same surface was extrapolated. Based on this calculation papillae on healthy skin had a mean surface of 650.4 ± 53.9 μm^2 with an effective diameter of 28.8 ± 8.9 µm. In psoriatic lesions we measured a mean surface of 3297.2 ± 402.6 μm^2 with an effective diameter of 64.2 ± 22.6 µm ($p<0.001$). The papillae diameter is almost double in size compared to healthy skin and in these dilated papillae is where the dilated blood vessels are located and supply with nutrients the fast growing keratinocytes. These results are summarized in Table 1.

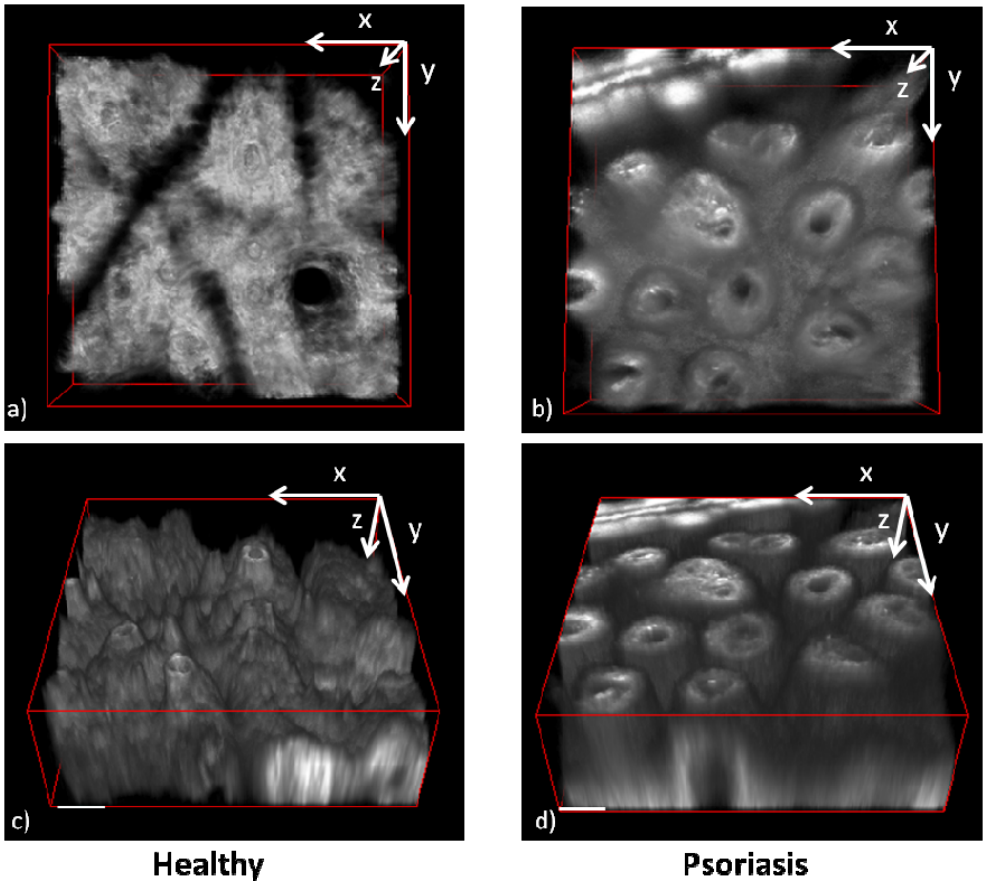

Fig. 5. 3D reconstruction of the dermal layer of healthy a),c) and psoriatic b),d) skin lesion. a) and b) the 3D volumes view is set to the x-y plane. c) and d) the volumes are rotated 30° in the y-z plane. c) The papillae in healthy skin are short, typically 30 µm and with small diameter around 29 µm. d) Psoriatic papillae dimensions are bigger with typical lengths more than 100 µm and a diameter of around 65 µm. (Scale bars: 50 µm).

#206234 - $15.00 USD Received 11 Feb 2014; revised 25 Apr 2014; accepted 28 Apr 2014; published 24 Jun 2014

Table 1. Summary of the measured vessel and papillae characteristics in psoriasis and healthy skin

Method	Feature	Healthy	Psoriasis
PMD	Vessel surface (μm^2)	532.4 ± 45.9	974.4 ± 40.5
	Effective vessel diameter (μm)	26.0 ± 7.6	35.2 ± 7.2
MM	Papilla surface (μm^2)	650.4 ± 53.9	3297.2 ± 402.6
	Effective papilla diameter (μm)	28.8 ± 8.9	64.2 ± 22.6

4. Discussion

One of the challenges in the dermatological clinical practice is the *in vivo* visualization of the morphology of skin with high contrast and high resolution. In present day, the microscopic morphology is unequivocally assessed *ex vivo* by performing histopathological examination of biopsy samples. We demonstrate the capability of using noninvasive means for the visualization of the skin morphology, with high contrast and resolution, dermoscopically and microscopically, in healthy and psoriatic skin and furthermore evaluate and quantify their differences.

Use of the PMD enables the visualization of the blood vessels and scattering characteristics with high contrast. Imaging of blood vessels is of particular interest for the case of psoriasis since it is an inflammatory disease where blood vessels proliferate in the epidermis and they have an increased size. Classical dermoscopy lacks specificity for hemoglobin absorption and therefore blood vessel contrast is low. Targeted illumination with the PMD and subsequent image processing produces images specific for hemoglobin absorption as seen in the Blood Contrast result in Fig. 2(e) where vessel patterns are clearly visualized. Segmentation of this image produces an image (Fig. 2(g)) with maximum contrast for hemoglobin from which the number and surface of superficial blood vessels can be measured. Analysis of this kind of images of psoriatic but also healthy skin revealed that psoriatic vessels are 83% bigger compared to those of healthy skin. Additionally the scattering characteristics of psoriatic lesions are imaged with high contrast in Fig. 2(f). The complete absence of wrinkle network is a demonstration of the inability of corneocytes to organize and form the structured layer of stratum corneum which is seen in healthy skin in Fig. 2(c). Moreover the identification of black parallel structures (Fig. 2(f)) has yet to be evaluated as a diagnostic criterion.

Microscopically the images acquired with the MM reveal *in vivo* the characteristic micro morphology of psoriasis. In the epidermis (Fig. 3) cells have very small cytoplasmic area and they are sparsely packed. Additionally, below the stratum corneum a region with a punctuated fluorescent pattern appears which is not visible in the healthy dermis. Characteristic also of psoriasis is the more pronounced epidermal proliferation and the dilated papillae of the dermis. Imaging in great depth of the epidermal proliferation is not possible because of the loss of signal due to increased scattering and absorption but imaging in depth of the papillae is possible due to their high SHG signal. Analysis of the 3D reconstruction (Fig. 5) reveals the big difference in morphology in psoriasis where the dilated and elongated papillae can be seen with high resolution. Analysis of the images reveals that papillae in psoriasis have a length of even more than 100 μm and a mean diameter of around 65 μm whereas in healthy skin these values are 30 μm and 29 μm correspondingly.

Measurements of capillaries and papillae diameter have also been performed with other techniques. With the method of capillaroscopy [24] the diameter of superficial psoriatic vessels was measured at 10.13 μm width, with 44.82 mm^{-1} density of vessels in the psoriatic lesion. Hegyi et al. [25] measured with Reflectance Confocal Microscopy (RCM) a variable size in capillary and papilla size with vessel diameter ranging from 16 μm to 140 μm with circularity values from 0.3 to 0.41, which only proves the variability of the vessel size in psoriatic lesions and their elliptic shape. Several other studies have been performed with RCM [19, 20, 26–29] in which the microscopic characteristics of psoriasis were investigated.

#206234 - $15.00 USD Received 11 Feb 2014; revised 25 Apr 2014; accepted 28 Apr 2014; published 24 Jun 2014

In most cases the investigation was based on the identification of pathologic morphologies such as parakeratosis, epidermal inflammatory cells, acanthosis, papillomatosis, and the count of dermal papillae that can be identified microscopically. In two separate studies with RCM in which papillae diameter were quantified, Ardigo et al. [27] reported values of papillae diameter of 151 μm for psoriasis and <90 μm for healthy skin and Archid et al. [29] reported values of 146 μm and 70 μm correspondingly. There is a significant difference when comparing with our results (64 μm psoriasis and 29 μm healthy). On the other hand, again based on RCM observations Wolberink et al. [28] measured the surface area of psoriatic papillae to be 4186.5 μm^2 in psoriatic lesions and 3095.8 μm^2 in uninvolved skin. Based on our method of calculation of the effective diameter, that would result to an effective diameter of 72 μm for psoriasis and 62 μm for uninvolved skin. In a recent RCM study Basaran et al. [19] measured dermal papillae diameter of 51 μm for psoriasis and 35 μm for uninvolved skin. These values [19, 28] are considerably different to the previous RCM studies [27, 29] and comparable to our findings. The great differences between studies could be attributed to the location of the body examined but most probably is related to the severity of the cases examined. We examined only lesions on the dorsal forearm and cases of psoriasis with similar clinical appearance and for this reason also the observed values of papillae diameter had a relative small variation. Moreover contrast mechanisms differ, in RCM contrast comes from backscattering of illumination light whereas in MM in the dermis contrast comes from the SHG from collagen fibers, therefore is specific for the connective tissue in papillae. In previous studies on psoriasis with MM [30, 31] differences between healthy and psoriatic skin were observed, however detailed description and quantification was not pursued. Additionally, imaging with Coherent anti-Stokes Raman scattering spectroscopy (CARS) revealed that lipids in the stratum corneum were decreased in psoriatic lesions [30], which is in accordance with the general observation that there are significant morphological and biochemical changes in the psoriatic corneum. In our study we focused mainly on the quantification of size parameters that could change after a potential treatment. What becomes clear though is that vessel diameter increases in psoriasis and furthermore it is possible to be measured. In the present study we have measured vessel size with a dermoscopic technique and papillae size with a more sophisticated microscopic technique. Moreover the images produced examine a lesion from different aspects, from the dermoscopic down to microscopic, offering a more complete view.

Imaging of psoriasis with such detail is not always required for performing diagnosis. However during the past years there has been an intensive effort in the research for the treatment of this disease [3, 32–34]. Since it is an autoimmune disease the target of the treatment is the deactivation of the immune component responsible for the immune reaction. Such therapies have risks and those risks could be reduced if the effect of a treatment can be timely assessed. Currently the severity of psoriasis is evaluated by the PASI index. The Psoriasis Area and Severity Index (PASI) [35] is used to assess the severity of psoriasis which constitutes of measuring, by visual inspection, the severity of erythema (redness), induration (thickness) and desquamation (scaling) in different parts of the body and assignment of a score accordingly. Subsequently the effect of a treatment is assessed based on the change of the PASI index. Apart from being subjective this methodology does not account for microscopic features such as blood vessel and papillae size which correlate to the severity of the inflammation. Monitoring of a potential treatment can be performed by visualization of the morphology of the epidermis and the dermis. In the epidermis, a possible index of the effect of a treatment could be the measure of the change of the nucleus to cytoplasm ratio, since the cytoplasmic area of the cells of spinous layer is very small compared to healthy skin. This ratio could serve as an index on the severity of psoriasis and its change rate could provide evidence on the effect of the treatment and the speed of its action. On the dermal layer, measurement of the papillae diameter and length can also be used as an index for the estimation of the effect of a treatment. Dermoscopically, measurement of the change of the

#206234 - $15.00 USD Received 11 Feb 2014; revised 25 Apr 2014; accepted 28 Apr 2014; published 24 Jun 2014

vessel diameter during the course of a treatment could provide an index on the clinical improvement of the lesion. Use of a PASI index which would include the microscopic and dermoscopic changes observed could provide a more objective and timely methodology for assessing the severity of psoriasis as well as assessing the effect of a treatment. Correlation of the measured values with the well-established PASI index during the course of a treatment could provide a means of comparison and evaluation of the proposed methodologies. Apart from monitoring the effect of an experimental treatment the *in vivo* techniques developed could be used for the personalization of existing treatments. It has been observed that although some systemic agents have impressive effects on some patients on some other have little success [36, 37]. In this case the developed methodologies could be used to estimate the effect of a specific treatment and help in selecting the most effective treatment for each patient. Very recently a study on treatment monitoring on psoriasis with RCM [19] successfully correlated the microscopic findings with the conventional PASI index. This shows that there is a correlation of microscopic observations with the clinical appearance of psoriasis. This also supports our proposal towards developing a PASI based on dermoscopic and microscopic observations which could offer objective assessment of a lesion.

5. Conclusions

Psoriasis is a skin disease with worldwide occurrence, however in most cases it is not life threatening. In the present study it was demonstrated the noninvasive *in vivo* imaging of psoriatic lesions. The characteristic morphological features were visualized with high detail and furthermore quantified. This supports the applicability of the PMD and MM for quantitative diagnostic purposes. Moreover it offers a possibility for employing the developed methodologies for monitoring the clinical improvement achieved after a treatment. Such methodologies could fulfill the need for successfully identifying and tailoring a personalized treatment for each patient.

Acknowledgments

The authors acknowledge the contribution of R. Ballerini, A. Hajeb (Mechanical Workshop of LENS), M. Giuntini, M. De Pas, A. Montuori (Electronic Workshop of LENS), on the microscope mechanics and electronics. The research leading to these results has received funding from the European Union Seventh Framework Programme (FP7/2007- 2013) under grant agreements n° 228334 (OptBio) and 284464 (Bioptichal) and from the Italian Ministry for Education, University and Research in the framework of the Flagship Project NANOMAX. D. Kapsokalyvas gratefully acknowledges funding from Marie Curie Host Fellowships Action for Early Stage Research Training ATLAS programme (MEST-CT-2004-008048). Financial support by the Ente Cassa di Risparmio di Firenze (private foundation) is acknowledged.

#206234 - $15.00 USD Received 11 Feb 2014; revised 25 Apr 2014; accepted 28 Apr 2014; published 24 Jun 2014